Effects of $1p_{3/2}$ and $0f_{5/2}$ hole excitations on N=50 isotones

1980 J. Phys. G: Nucl. Phys. 6 345

(http://iopscience.iop.org/0305-4616/6/3/010)

J. Phys. G: Nucl. Phys. 6 (1980) 345–357. Printed in Great Britain

Effects of $1p_{3/2}$ and $0f_{5/2}$ hole excitations on $N = 50$ isotones†

H C Chiang‡, M C Wang‡ and C S Han§

‡ Department of Physics, National Tsing Hua University, Hsinchu, Taiwan, Republic of China

§ Department of Electrophysics, National Chiao Tung University, Hsinchu, Taiwan, Republic of China

Received 14 August 1979, in final form 8 October 1979

Abstract. The effects of the $1p_{3/2}$ and $0f_{5/2}$ one-hole excitations are examined for $N = 50$ isotones. The pseudo-nucleus ^{100}Sn is assumed to be the inert core and a two-range central-plus-tensor potential is used for the effective interaction. It is found that the calculated low-lying energy spectra agree with the experimental data quite well. Many more states can be accommodated by expansion of the model space. The transition probabilities are calculated. It is found that inclusion of $1p_{3/2}$ and $0f_{5/2}$ hole excitations in general improves the agreement between the calculated transition probabilities and experimental data.

1. Introduction

Many calculations have been reported on the low-energy spectra and electromagnetic transition probabilities of $N = 50$ isotones (Bayman *et al* 1959, Cohen *et al* 1964, Talmi and Unna 1960, Auerbach and Talmi 1965, Vervier 1966, Ball *et al* 1972, Gloeckner *et al* 1972, Gloeckner and Serduke 1974, Chiang *et al* 1978). In previous calculations, the nucleus ^{88}Sr is taken as the inert core and the neutron orbits are assumed to be closed. The $Z - 38$ protons are assumed to occupy the $1p_{1/2}$ and $0g_{9/2}$ orbitals. The low-lying energy spectra and some electromagnetic transition rates are calculated using suitable interactions. Generally speaking, the agreement between the calculated and experimental results is quite good. However, it was pointed out that some low-lying levels cannot be accommodated in this size of model space (Hughes 1969, Dedes and Irvine 1975, Fujita and Komoda 1978). Hughes calculated the negative-parity states for ^{91}Nb by expanding the model space to include $1p_{3/2}$ and $0f_{5/2}$ hole excitations. The resultant wavefunctions were used by Schäfer and Rauch (1977) to calculate the transition probabilities of the negative-parity states of ^{91}Nb, and improved results were obtained. Dedes and Irvine (1975) calculated the positive-parity states of ^{90}Zr by including the $1p_{3/2}$ and $0f_{5/2}$ excitations to the $0g_{9/2}$ orbit. 'Sussex' and 'Yale' interactions were used to produce the energy spectra. It was found that the level spacings of the exited states agreed reasonably well with the experimental results but the ground state was predicted much too low. Fujita and Komoda (1978) extended the model space to include one- or two-hole excitations from the $1p_{3/2}$ orbit. The Kallio–Kolltveit interaction was adopted and the energy spectra and transition probabilities of the $N = 50$ isotones were calculated. Reasonable agreement between the calculated and observed energy spectra was obtained. In the calculation of electromagnetic transition probabilities some distinct improvements were obtained.

†Work supported by the National Science Council, Republic of China.

0305-4616/80/030345 + 13$01.50

It was pointed out that the inclusion of the $0f_{5/2}$ orbit may produce considerable effect even for some low-lying states (Schäfer and Rauch 1977, Fujita and Komoda 1978). The relatively large effective charge needed to fit the electromagnetic transition probabilities also suggests that further expansion of the model space is needed. In the past few years many new experimental data on the $N = 50$ isotones have become available. Therefore, it is considered that it might be proper at this stage to make a more extensive analysis of the effects of $1p_{3/2}$ and $0f_{5/2}$ orbitals by comparing with the more abundant experimental data for the $N = 50$ isotones. In this work, we report some results of such a calculation. Since quite a lot of new experimental data on the energy levels with certain J^π assignments is available, we perform a least-squares-fit calculation on the energy levels of $N = 50$ isotones in the extended model space. The resultant wavefunctions are used to calculate the electromagnetic transition probabilities. The result for the smaller model space in which the $1p_{3/2}$ and $0f_{5/2}$ excitations are suppressed is also calculated for comparison. In § 2 details of our model calculation are described. In § 3 the resultant interaction is discussed. In §§ 4 and 5 the results for the energy spectra and electromagnetic transition probabilities are reported. Finally we briefly present our conclusions.

2. The model

In this calculation, the pseudo-nucleus ^{100}Sn is assumed to be the inert core. Therefore, we assume that the neutron shell is closed and the $50 - Z$ proton holes are distributed among the $1p_{3/2}$, $0f_{5/2}$, $1p_{1/2}$ and $0g_{9/2}$ orbitals. However, in order to reduce the calculation to feasible proportions, we restrict our considerations to the one-hole excitations in the $1p_{3/2}$ and $0f_{5/2}$ orbitals.

For the effective interactions, a two-range central-plus-tensor potential is assumed. The radial part of the potential is assumed to be of Yukawa type. The short-range part is assumed to be the pion Compton wavelength as adopted in most other calculations which use a similar potential. The long-range potential components are included to mediate the core polarisation effects. From previous calculations it was shown that the quality of fit does not depend on the specific value of the second range very sensitively, and its value is tentatively assumed to be 2 fm (Moinester *et al* 1969, Anantaraman and Schiffer 1971, Schiffer and True 1976, King Yen *et al* 1977).

In the calculation harmonic oscillator wavefunctions are used for the single-particle wavefunctions. As usual, the oscillation parameter is assumed to be mass dependent with the relation $\nu = 0{\cdot}96 \times A^{-1/3}\,\mathrm{fm}^{-2}$. In this calculation the average A value is chosen to be 90.

With these specifications we carried out a least-squares-fit calculation on the low-lying energy spectra of $N = 50$ isotones. Since in our model the binding energies and Coulomb displacement correlations are not available, only the excitation energies relative to the corresponding ground-state energies are calculated. In the input experimental data 83 excited low-lying levels with known J^π assignments are included in the calculation. There are six $T = 1$ interaction components, i.e. the central singlet-even, triplet-odd and tensor-odd components of both ranges. From previous calculations the long-range tensor-odd component is not as important as the other components. We therefore omit this component in order to reduce the number of parameter. The five interaction parameters and the $1p_{1/2}$–$0g_{9/2}$, $1p_{3/2}$–$0g_{9/2}$ and $0f_{5/2}$–$0g_{9/2}$ single-particle level spacings are varied until the discrepancy between the calculated and observed energy levels is minimised. In order to see the effects of the $1p_{3/2}$ and $0f_{5/2}$ hole excitations the result of the smaller model space in which the $1p_{3/2}$ and $0f_{5/2}$ orbitals are omitted is

also presented for comparison. In this part of calculation those states that do not have a model-space analogue are naturally omitted. Also excluded are the $1p_{3/2}$–$0g_{9/2}$ and $0f_{5/2}$–$0g_{9/2}$ single-particle level spacings. The resultant wavefunctions are used to calculate the electromagnetic transition probabilities. The calculated transition probabilities are compared with available experimental data.

3. Effective interactions

The best-fit potential strength parameters for model space I (without $1p_{3/2}$ and $0f_{5/2}$ excitations) and model space II (with $1p_{3/2}$ and $0f_{5/2}$ excitations) are displayed in table 1. The two sets of parameters are qualitatively very similar. The short-range central singlet-even (CSE) and triplet-odd (CTO) components are all attractive while the corresponding long-range components are repulsive. The tensor triplet-odd (TTO) components are repulsive but the value in model space I is much larger. In the column ST the potential parameters determined directly from the experimental diagonal two-body matrix elements over the whole nuclear chart by Schiffer and True (1976) are also displayed for comparison. It seems the values of model space II in general lie in between those of model space I and those of Schiffer and True. The only exception is the long-range singlet-even component. The strength of this component is comparatively weaker. Since the inclusion of the long-range component is to mediate the core polarisation effects, we expect that the need for the long-range component should be reduced in the case of model space II. This might serve as an explanation for the weak contribution from the long-range singlet-even component. The best-fit $0g_{9/2}$–$1p_{1/2}$ single-particle level spacing for the calculation in model space I is 1·2 MeV and the best-fit $0g_{9/2}$–$1p_{1/2}$, $0g_{9/2}$–$1p_{3/2}$ and $0g_{9/2}$–$0f_{5/2}$ level spacings for model space II are 0·7, 1·97 and 4·79 MeV respectively.

The two-body matrix elements calculated using the best-fit potentials are displayed in tables 2 and 3. In table 2 we present those two-body matrix elements which are related to the $0g_{9/2}$ and $1p_{1/2}$ orbitals. It is very interesting to notice that the two-body matrix elements determined from the best-fit potentials of model space I and model space II are very similar. This suggests that even if the potential parameters and single-particle levels spacings are model-space dependent, this does not rule out the universality of the two-body matrix elements conjectured by Moinester *et al* (1969), Anantaraman and Schiffer (1971) and Schiffer and True (1976). Also displayed in table 2 are those matrix elements determined in other least-squares-fit calculations in which the two-body matrix elements are used as variable parameters. The matrix elements determined by Gloeckner and Serduke (1974) and Ball *et al* (1972) are displayed in the columns specified by GS

Table 1. Best-fit potential parameters for model spaces I and II. The parameters determined by Schiffer and True are shown in the column specified by ST for comparison.

Short range	I	II	ST
CSE	−99·86	−65·70	−49·92
CTO	−217·32	−196·62	−155·82
TTO	19·0	4·24	−6·10
Long range	**I**	**II**	**ST**
CSE	28·56	9·04	15·47
CTO	91·36	83·90	62·06

Table 2. Best-fit two-body matrix elements of $0g_{9/2}$ and $1p_{1/2}$ orbitals.

$2j_1$	$2j_2$	$2j_3$	$2j_4$	j	I	II	GS	BML	KB
1	1	1	1	0	−0·497	−0·660	−0·542	−0·484	−0·249
1	1	9	9	0	0·630	0·615	0·853	0·901	0·650
1	9	1	9	4	0·381	0·440	0·714	0·690	—
1	9	1	9	5	−0·023	−0·097	0·195	0·175	—
9	9	9	9	0	−2·206	−2·077	−1·707	−1·719	−1·147
9	9	9	9	2	−0·735	−0·773	−0·613	−0·603	−0·852
9	9	9	9	4	−0·156	−0·195	0·144	0·164	−0·259
9	9	9	9	6	0·084	0·059	0·450	0·508	−0·037
9	9	9	9	8	0·336	0·323	0·565	0·570	0·094

Table 3. Best-fit two-body matrix elements related to $1p_{3/2}$ and $0f_{5/2}$ excitations.

$2j_1$	$2j_2$	$2j_3$	$2j_4$	j	This work (II)
9	5	9	5	2	0·029
9	5	9	5	3	0·164
9	5	9	5	4	0·404
9	5	9	5	5	−0·018
9	5	9	5	6	0·425
9	5	9	5	7	−1·081
9	3	9	3	3	−0·702
9	3	9	3	4	0·223
9	3	9	3	5	0·172
1	5	1	5	2	−0·239
1	5	1	5	3	0·403
1	3	1	3	1	0·459
1	3	1	3	2	−0·975
9	9	1	5	2	0·355
9	9	1	3	2	0·277
9	1	9	5	4	−0·024
9	5	9	3	3	0·242
9	5	9	3	4	0·009
9	5	9	3	5	0·215
9	5	9	3	6	0·018
9	1	9	3	4	0·162
9	1	9	3	5	0·615
1	5	1	3	2	−0·237

and BML respectively. The values agree qualitatively with those obtained in this work. In the last column of table 2 some matrix elements calculated by Kuo and Brown (1968) are also shown for comparison. The two-body matrix elements related to the $1p_{3/2}$ and $0f_{5/2}$ excitations are shown in table 3 for reference. There are some matrix elements with quite large strengths. This suggests that the expansion of the model space is really necessary.

4. Energy spectra

The calculated and experimental energy spectra are shown in figures 1 and 2 for comparison. In the figures the results with model space I and model space II are denoted as I and II respectively. Those levels that cannot be explained in our model space or have

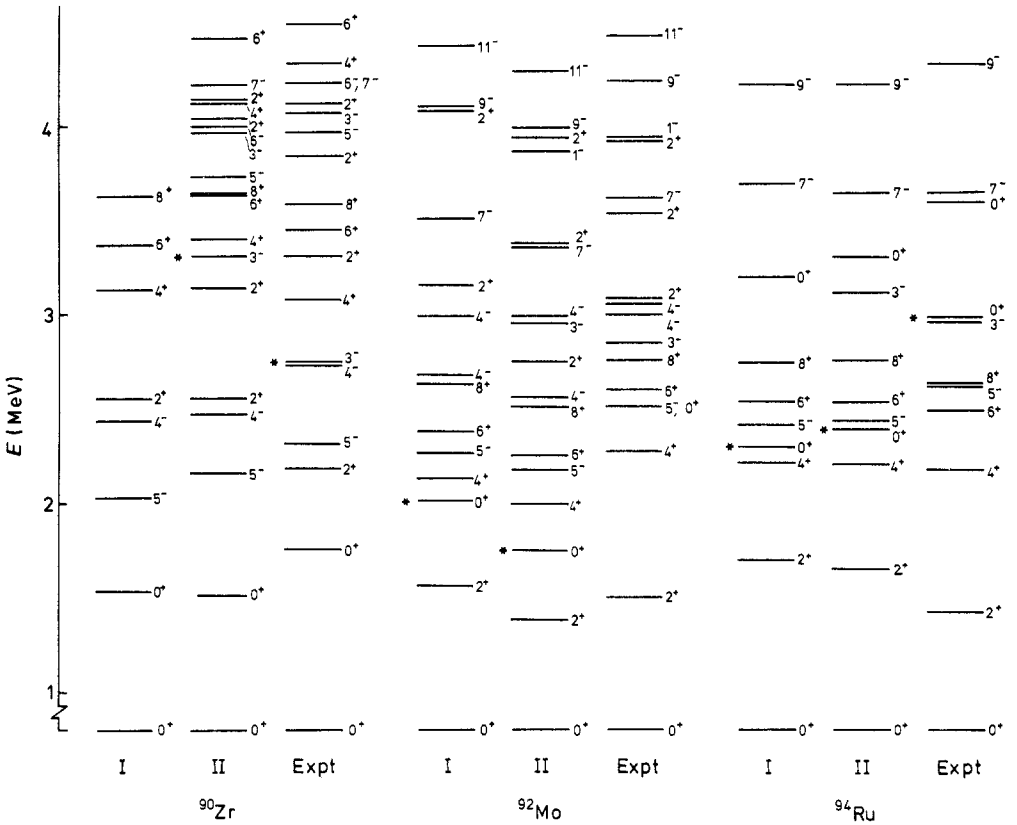

Figure 1. Experimental and calculated energy spectra for even $N = 50$ isotones. The experimental data for ^{90}Zr are adopted from Glickstein *et al* (1971), Stooksberry *et al* (1976) and Beshai *et al* (1978). The experimental data for ^{92}Mo are adopted from Papadopoulos *et al* (1975), Metzger (1977) and Lederer *et al* (1971). The experimental data for ^{94}Ru are adopted from Lederer *et al* (1971).

uncertain J^π assignments are excluded from the least-squares fit and are marked by an asterisk. Generally speaking, the low-lying spectra of sets I and II are quite similar and agree quite well with the experimental values. However, many more states can be reproduced in the set II calculation. The overall root-mean-square deviation for 56 levels in the set I calculation is 0·20 MeV and the corresponding value for 83 levels in the set II calculation is 0·22 MeV. This means that the expansion of the model space does not improve the quality of fit, but can accommodate many more states.

The energy spectra for even-mass isotones are shown in figure 1. In the case of ^{90}Zr the spectra of sets I and II below the first 8^+ state are very similar. However, nine more states, i.e. the 2_2^+, 2_3^+, 2_4^+, 4_2^+, 6_2^+ 3_2^-, 5_2^-, 6_1^-, 7_1^- states, can be reproduced in the set II calculation. All of these states have strong $1p_{3/2}$ or $0f_{5/2}$ admixtures as expected. The major intensity distributions are shown in table 4. We found that the 4_2^+, 5_2^-, 6_2^+ states are dominated by $1p_{3/2}$ hole excitation while the 3_2^-, 6_1^-, 7_1^- states are dominated by $0f_{5/2}$ hole excitation. The 2_3^+ and 2_4^+ states are strong mixtures of $1p_{3/2}$ and $0f_{5/2}$ excitations. The 2_2^+ state is a mixture of $|(\frac{9}{2})^{-8}(\frac{1}{2})^{-2}\rangle$ and $|(\frac{9}{2})^{-8}(\frac{1}{2})^{-1}(\frac{3}{2})^{-1}\rangle$ configurations. However, in the set I calculation this state cannot be reproduced since there is only one 2^+ state in the model space. The $1p_{3/2}$ and $0f_{5/2}$ excitations have smaller effects on the energy spectra of ^{92}Mo. Experimentally there are four 2^+ states below an excitation

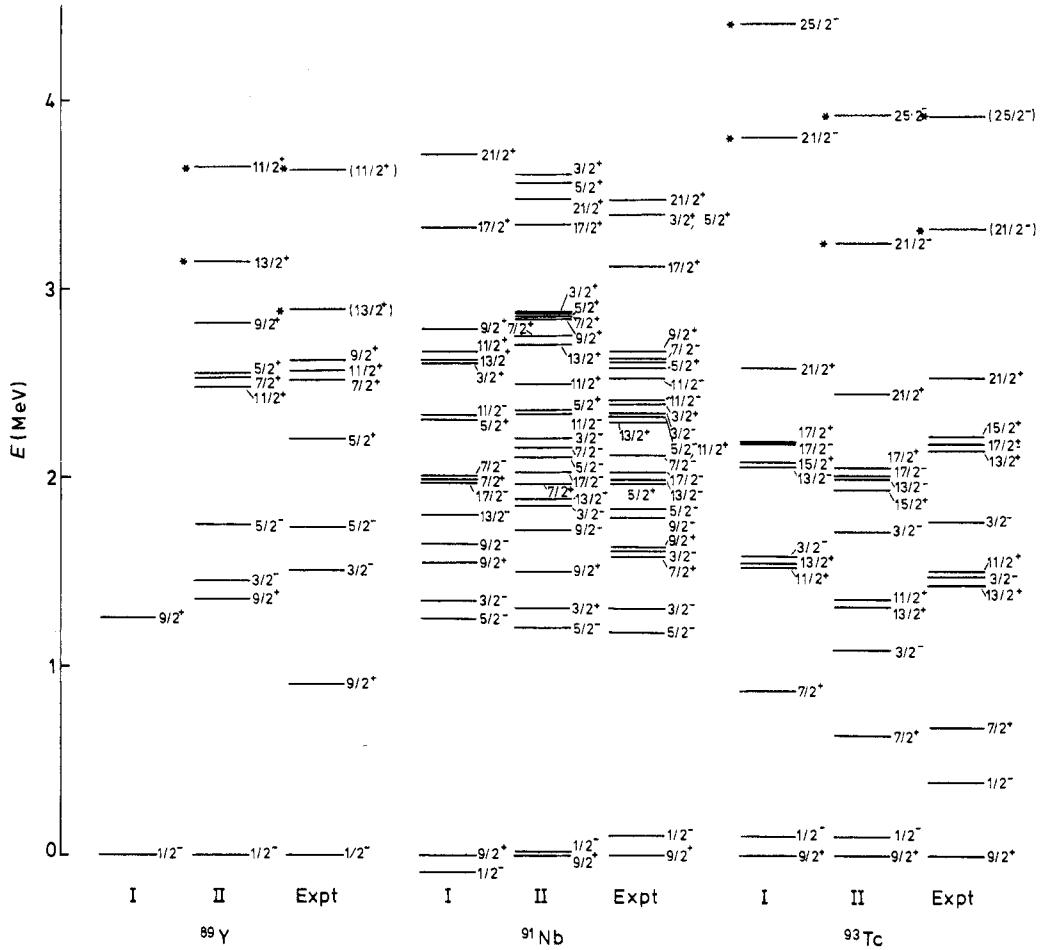

Figure 2. Experimental and calculated energy spectra for odd $N = 50$ isotones. The experimental data for ^{89}Y are adopted from Fivozinsky *et al* (1974) and Hulstman *et al* (1975). The experimental data for ^{91}Nb are adopted from Schäffer and Rauch (1977), Horton *et al* (1972) and Thornton *et al* (1976). The experimental data for ^{93}Tc are adopted from Riley *et al* (1971), Grecescu *et al* (1973) and Shamai *et al* (1972).

Table 4. The wavefunction intensity distributions of those states of ^{90}Zr which have strong $1p_{3/2}$ and $0f_{5/2}$ admixtures.

State	Configuration (intensity)
2_2^+	$\|(\frac{9}{2})^{-8}(\frac{1}{2})^{-2}\rangle(0{\cdot}51)$ $\|(\frac{9}{2})^{-8}(\frac{1}{2})^{-1}(\frac{3}{2})^{-1}\rangle(0{\cdot}42)$
2_3^+	$\|(\frac{9}{2})^{-8}(\frac{1}{2})^{-1}(\frac{3}{2})^{-1}\rangle(0{\cdot}40)$ $\|(\frac{9}{2})^{-8}(\frac{1}{2})^{-1}(\frac{5}{2})^{-1}\rangle(0{\cdot}57)$
2_4^+	$\|(\frac{9}{2})^{-8}(\frac{1}{2})^{-1}(\frac{3}{2})^{-1}\rangle(0{\cdot}68)$ $\|(\frac{9}{2})^{-8}(\frac{1}{2})^{-1}(\frac{5}{2})^{-1}\rangle(0{\cdot}29)$
4_2^+	$\|(\frac{9}{2})^{-8}(\frac{1}{2})^{-1}(\frac{3}{2})^{-1}\rangle(0{\cdot}93)$
6_2^+	$\|(\frac{9}{2})^{-8}(\frac{1}{2})^{-1}(\frac{3}{2})^{-1}\rangle(0{\cdot}91)$
3_2^-	$\|(\frac{9}{2})^{-7}(\frac{1}{2})^{-2}(\frac{5}{2})^{-1}\rangle(0{\cdot}69)$ $\|(\frac{9}{2})^{-9}(\frac{5}{2})^{-1}\rangle(0{\cdot}25)$
5_2^-	$\|(\frac{9}{2})^{-7}(\frac{1}{2})^{-2}(\frac{3}{2})^{-1}\rangle(0{\cdot}95)$
6_1^-	$\|(\frac{9}{2})^{-9}(\frac{5}{2})^{-1}\rangle(0{\cdot}90)$
7_1^-	$\|(\frac{9}{2})^{-9}(\frac{5}{2})^{-1}\rangle(0{\cdot}98)$

energy of 4 MeV. In the model space I there are only three 2^+ states. In the model space II all four 2^+ states can be reproduced. In this case all 2^+ states, except for the lowest one, have strong $1p_{3/2}^{-1}$ components. The major intensities for the 2_2^+ state are 0·36 and 0·52 for $|(\frac{9}{2})^{-6}(\frac{1}{2})^{-2}\rangle$ and $|(\frac{9}{2})^{-7}(\frac{3}{2})^{-1}\rangle$ respectively. The 2_3^+ state has the same major components as the 2_2^+ state, but the corresponding distributions are 0·50 and 0·40 respectively. The 2_4^+ state is mainly a mixture of $|(\frac{9}{2})^{-6}(\frac{1}{2})^{-2}\rangle$ and $|(\frac{9}{2})^{-6}(\frac{1}{2})^{-1}(\frac{3}{2})^{-1}\rangle$ with intensity 0·40 for each configuration. The 1^- state at 3·944 MeV excitation energy can be reproduced quite well. It is almost a pure $0f_{5/2}$ hole state with an intensity of 0·87 for the $|(\frac{9}{2})^{-6}(\frac{1}{2})^{-1}(\frac{5}{2})^{-1}\rangle$ configuration. Another interesting state worthy of mention is the 3_1^- state. This state can be reproduced quite well with the major components being $|(\frac{9}{2})^{-7}(\frac{1}{2})^{-1}\rangle(0{\cdot}50)$ and $|(\frac{9}{2})^{-7}(\frac{3}{2})^{-1}\rangle(0{\cdot}47)$. Our calculation suggests that the structure of this state might not be so complicated as conjectured in previous calculations (Fujita and Komoda 1978). The 0_2^+ state cannot be reproduced. The calculated position is far too low compared with the experimental value. Note that this level can be reproduced in previous least-squares-fit calculations in which the matrix elements are used as free parameters (Gloeckner and Serduke 1974, Ball *et al* 1972). However, we would like to mention that Ball *et al* did find that there was incompatibility between low-lying 0^+ states and high-spin negative-parity states. The calculated energy spectra of ^{94}Ru for model spaces I and II are very similar. Again the second 0^+ state cannot be fitted well. The 3_1^- state at an excitation energy of 2·95 MeV can be reproduced. The major intensity of this state is 0·71 for the $|(\frac{9}{2})^{-5}(\frac{3}{2})^{-1}\rangle$ configuration.

The energy spectra of odd-mass isotones are shown in figure 2. The energy spectrum of ^{89}Y is strongly affected by including the $1p_{3/2}$ and $0f_{5/2}$ excitations. Except for the $\frac{9}{2}_1^+$ state, all other states do not have a model-space analogue in the set I calculation. The leading intensity distributions for these states are shown in table 5. The configuration distribution for the $\frac{3}{2}_1^-$ state is a mixture of $|(\frac{9}{2})^{-10}(\frac{3}{2})^{-1}\rangle(0{\cdot}64)$ and $|(\frac{9}{2})^{-8}(\frac{1}{2})^{-2}(\frac{3}{2})^{-1}\rangle(0{\cdot}35)$ while other states seem to have a rather pure distribution. It is interesting to point out that the $\frac{5}{2}_1^-$ and $\frac{11}{2}_2^+$ states are dominated by $0f_{5/2}$ excitation and therefore cannot be reproduced by previous calculations in which the $0f_{5/2}$ excitation is omitted (Fujita and Komoda 1978). The energy spectrum of ^{91}Nb is strongly influenced by expansion of the model space. Eight more states with known J^π assignments can be reproduced. These states are $\frac{3}{2}_2^+$, $\frac{5}{2}_2^+$, $\frac{5}{2}_3^+$, $\frac{7}{2}_2^+$, $\frac{3}{2}_2^-$, $\frac{3}{2}_3^-$, $\frac{5}{2}_2^-$ and $\frac{7}{2}_2^-$. All of them are dominated by $1p_{3/2}$ and $0f_{5/2}$ excitations. The major intensity distributions are shown in table 6. The low-lying $\frac{5}{2}_2^-$ state at 1·85 MeV is dominated by $0f_{5/2}$ excitation with an intensity of 0·90. This is in agreement with the calculation of Hughes (1969) and the results of transfer reactions (Chapman *et al* 1972) and the γ-ray transition (Schäfer and Rauch 1977). Schäfer and

Table 5. The wavefunction intensity distributions of those states of ^{89}Y which have strong $1p_{3/2}$ and $0f_{5/2}$ admixtures.

State	Configuration (intensity)
$\frac{5}{2}_1^+$	$\|(\frac{9}{2})^{-9}(\frac{1}{2})^{-1}(\frac{3}{2})^{-1}\rangle(0{\cdot}99)$
$\frac{7}{2}_1^+$	$\|(\frac{9}{2})^{-9}(\frac{1}{2})^{-1}(\frac{3}{2})^{-1}\rangle(0{\cdot}93)$
$\frac{9}{2}_2^+$	$\|(\frac{9}{2})^{-9}(\frac{1}{2})^{-1}(\frac{3}{2})^{-1}\rangle(0{\cdot}92)$
$\frac{11}{2}_1^+$	$\|(\frac{9}{2})^{-9}(\frac{1}{2})^{-1}(\frac{3}{2})^{-1}\rangle(0{\cdot}95)$
$\frac{11}{2}_2^+$	$\|(\frac{9}{2})^{-9}(\frac{1}{2})^{-1}(\frac{5}{2})^{-1}\rangle(0{\cdot}94)$
$\frac{13}{2}_1^+$	$\|(\frac{9}{2})^{-9}(\frac{1}{2})^{-1}(\frac{3}{2})^{-1}\rangle(0{\cdot}95)$
$\frac{3}{2}_1^-$	$\|(\frac{9}{2})^{-10}(\frac{3}{2})^{-1}\rangle(0{\cdot}64)$ $\|(\frac{9}{2})^{-8}(\frac{1}{2})^{-2}(\frac{3}{2})^{-1}\rangle(0{\cdot}35)$
$\frac{5}{2}_1^-$	$\|(\frac{9}{2})^{-10}(\frac{5}{2})^{-1}\rangle(0{\cdot}97)$

Table 6. The wavefunction intensity distributions of those states of ^{91}Nb which have strong $1p_{3/2}$ and $0f_{5/2}$ admixtures.

State	Configuration (intensity)
$\frac{3}{2}^+_2$	$\|(\frac{9}{2})^{-7}(\frac{1}{2})^{-1}(\frac{3}{2})^{-1}\rangle(0{\cdot}88)$
$\frac{5}{2}^+_2$	$\|(\frac{9}{2})^{-7}(\frac{1}{2})^{-2}\rangle(0{\cdot}54)\ \|(\frac{9}{2})^{-7}(\frac{1}{2})^{-1}(\frac{3}{2})^{-1}\rangle(0{\cdot}37)$
$\frac{5}{2}^+_3$	$\|(\frac{9}{2})^{-7}(\frac{1}{2})^{-1}(\frac{3}{2})^{-1}\rangle(0{\cdot}94)$
$\frac{7}{2}^+_2$	$\|(\frac{9}{2})^{-7}(\frac{1}{2})^{-1}(\frac{3}{2})^{-1}\rangle(0{\cdot}77)$
$\frac{3}{2}^-_2$	$\|(\frac{9}{2})^{-8}(\frac{1}{2})^{-1}\rangle(0{\cdot}45)\ \|(\frac{9}{2})^{-6}(\frac{1}{2})^{-2}(\frac{3}{2})^{-1}\rangle(0{\cdot}52)$
$\frac{3}{2}^-_3$	$\|(\frac{9}{2})^{-6}(\frac{1}{2})^{-2}(\frac{3}{2})^{-1}\rangle(0{\cdot}94)$
$\frac{5}{2}^-_2$	$\|(\frac{9}{2})^{-8}(\frac{5}{2})^{-1}\rangle(0{\cdot}90)$
$\frac{7}{2}^-_2$	$\|(\frac{9}{2})^{-8}(\frac{3}{2})^{-1}\rangle(0{\cdot}89)$

Rauch have also found that the transition from $\frac{5}{2}^+_2$ to $\frac{7}{2}^+$ states is mainly M1 radiation and therefore suggested that the $\frac{5}{2}^+_2$ state at 2·58 MeV should have some $(p_{3/2})^{-1}$ component. Our result shows that this state has the intensity 0·37 for the configuration $|(g_{9/2})^{-7}(p_{1/2})^{-1}(p_{3/2})^{-1}\rangle$. The energy spectrum of ^{93}Tc is influenced slightly by expansion of the model space. There are two observed $\frac{3}{2}^-$ states. In the model space I only one $\frac{3}{2}^-$ state can be reproduced, while both of them can be reproduced in model space II. However, analysis of the wavefunctions indicates that the first $\frac{3}{2}^-$ state is dominated by the $|(\frac{9}{2})^{-6}(\frac{3}{2})^{-1}\rangle$ configuration (0·7) while the second $\frac{3}{2}^-$ state is dominated by the $|(\frac{9}{2})^{-6}(\frac{1}{2})^{-1}\rangle$ configuration (0·81). This suggests that the $\frac{3}{2}^-$ state obtained in the model space I calculation should be assigned to the second observed $\frac{3}{2}^-$ state.

5. Transition probabilities

The wavefunctions obtained in the least-squares-fit calculation are used to calculate the transition probabilities. The calculated transition probabilities are displayed in tables 7–11. Since experimental data on the transition probabilities are meagre and the discrepancies between the calculated and observed values are quite dispersive, it might not be very meaningful to determine an 'average' effective charge or g factor. Furthermore, the effects of $1p_{3/2}$ and $0f_{5/2}$ hole excitations may be masked by introducing the effective charge. Therefore, a free proton charge and g factor are employed in the calculations and the results corresponding to the set I and set II calculations are compared with each other and with the experimental data when available.

The transition probabilities of ^{90}Zr are displayed in table 7. It can be seen that the transition probabilities are enhanced by including the $1p_{3/2}$ and $0f_{5/2}$ excitations. In particular, there are transitions which are forbidden in model space I but not in model space II. Some transitions which involve those states that can only be reproduced in model space II are also calculated for reference. The calculated E2 reduced transition probability between the 2^+_1 and 0^+_1 states is much too small compared with the observed values (Kocher 1975, Singhal *et al* 1974). The calculations of Fujita and Komoda with $(1p_{3/2})^2$ excitations also have similar discrepancies. The calculated E3 and E4 transition probabilities in the set II calculation seem to fit the available experimental data reasonably well. The calculated E5 transition probabilities between 5^-_1 and 0^+_1 states are too small compared with the experimental data (Bauer *et al* 1973). The improvement in the set II calculation is by no means enough to make up the discrepancies.

The transition probabilities of ^{92}Mo are shown in table 8. The calculated M1 transition probabilities between the 2^+_2 and 2^+_1 states are too small compared with the observed

Table 7. Experimental and calculated electromagnetic transition probabilities of ^{90}Zr. $B(E, L)$ values are given in units of $e^2\,\mathrm{fm}^{2L}$ and $B(M, L)$ values are given in units of $\mu_0^2\,\mathrm{fm}^{2(L-1)}$.

Type	$J_i \rightarrow J_f$	$B(\sigma, L)_I$	$B(\sigma, L)_{II}$	$B(\sigma, L)_{exp}$
M1	$4_1^- \rightarrow 5_1^-$	0·10	0·14	
	$2_2^+ \rightarrow 2_1^+$	—	$7{\cdot}5 \times 10^{-3}$	
	$6_1^- \rightarrow 5_2^-$	—	$1{\cdot}2 \times 10^{-3}$	
E2	$2_1^+ \rightarrow 0_1^+$	26·59	39·31	135[a]
	$4_1^+ \rightarrow 2_1^+$	26·40	52·81	
	$2_2^+ \rightarrow 0_1^+$	—	0·24	
	$6_1^+ \rightarrow 4_1^-$	24·59	30·95	
	$6_2^+ \rightarrow 4_1^+$	—	11·91	
	$8_1^+ \rightarrow 6_1^+$	10·85	8·52	$60{\cdot}5 \pm 2{\cdot}5$[b]
	$6_1^- \rightarrow 4_1^-$	—	0·20	
	$7_1^- \rightarrow 5_2^-$	—	59·15	
E3	$3_1^- \rightarrow 0_1^+$	0·0	$8{\cdot}76 \times 10^2$	$15{\cdot}4 \times 10^3$[d]
	$8_1^+ \rightarrow 5_1^-$	0·0	22·4	31 ± 3[e]
	$5_1^- \rightarrow 2_1^+$	—	4·70	
	$5_2^- \rightarrow 2_1^+$	—	81·34	
E4	$4_1^+ \rightarrow 0_1^+$	$1{\cdot}4 \times 10^4$	$2{\cdot}34 \times 10^4$	$3{\cdot}8 \times 10^4$[c]
	$7_1^- \rightarrow 3_1^-$	—	$6{\cdot}56 \times 10^3$	
E5	$5_1^- \rightarrow 0_1^+$	$1{\cdot}34 \times 10^5$	$2{\cdot}05 \times 10^5$	$3{\cdot}3 \times 10^7$[f]
	$5_1^- \rightarrow 0_2^+$	$1{\cdot}07 \times 10^6$	$1{\cdot}40 \times 10^6$	
	$5_2^- \rightarrow 0_1^+$	—	$5{\cdot}35 \times 10^5$	
	$5_2^- \rightarrow 0_2^+$	—	$8{\cdot}89 \times 10^3$	

[a]Kocher (1975) and Singhal *et al* (1974); [b]Löbner (1964); [c]Ho *et al* (1973); [d]Bellicard *et al* (1970); [e]Tucker and Simmons (1970); [f]Bauer *et al* (1973).

value (Papadopoulos *et al* 1975). As in the case of ^{90}Zr, the calculated E2 transition probabilities between the 2^+ and 0^+ states are also too small compared with the experimental values (Stelson and Grodzins 1965). The inclusion of $1p_{3/2}$ and $0f_{5/2}$ one-hole excitations seems to help very little in these transitions. Other calculated E2 transitions seem to agree with the experimental data reasonably well. Except for E3 transitions, which are forbidden in model space I, the results of calculations I and II are very similar. This is in agreement with the result that the calculated energy spectra of set I and set II calculations are very similar. The 1^- state at an excitation energy of 3·94 MeV is almost a pure $0f_{5/2}$ hole state. Some transitions involving this state are also calculated for reference.

The transition probabilities of ^{94}Ru are listed in table 9. It can be seen from the table that the transition probabilities of calculations I and II are very similar. The major differences are in the E3 transitions that are forbidden in model space I. It is known that the $8_1^+ \rightarrow 6_1^+$ and $6_1^+ \rightarrow 4_1^+$ E2 transition probabilities are much smaller compared with the corresponding transitions in ^{90}Zr and ^{92}Mo (Lederer *et al* 1971). The calculated results for the $8_1^+ \rightarrow 6_1^+$ and $6_1^+ \rightarrow 4_1^+$ transitions are approximately one order too large. This is contrary to the usual tendency that the calculated transition probabilities are smaller than the observed ones. This means that an effective charge much smaller than unity is needed in order to fit the calculated $8_1^+ \rightarrow 6_1^+$ and $6_1^+ \rightarrow 4_1^+$ transition probabilities with the experimental values. Furthermore, the inclusion of $1p_{3/2}$ and $0f_{5/2}$ excitations does not improve the calculated results. Further investigations are needed to account for the discrepancies.

The only available calculated transition of ^{89}Y in model space I is the $\frac{9}{2}_1^+ \rightarrow \frac{1}{2}_1^-$ M4

Table 8. Experimental and calculated electromagnetic transition probabilities of ^{92}Mo.

Type	$J_i \to J_f$	$B(\sigma, L)_I$	$B(\sigma, L)_{II}$	$B(\sigma, L)_{exp}$
M1	$4_1^- \to 5_1^-$	$7{\cdot}4 \times 10^{-2}$	$9{\cdot}9 \times 10^{-2}$	
	$2_2^+ \to 2_1^+$	0·0	$5{\cdot}36 \times 10^{-5}$	$6{\cdot}3 \times 10^{-2}$ [a]
E2	$2_1^+ \to 0_1^+$	33·41	52·87	234 ± 40 [b]
	$2_2^+ \to 0_1^+$	4·08	4·90	75^{+22}_{-54} [a]
	$4_1^+ \to 2_1^+$	38·70	85·36	<583 [a]
	$0_2^+ \to 2_1^+$	20·31	22·02	
	$6_1^+ \to 4_1^+$	22·16	41·19	$78{\cdot}5 \pm 2{\cdot}5$ [c]
	$8_1^+ \to 6_1^+$	30·18	49·70	$32{\cdot}41 \pm 1{\cdot}2$ [c]
	$7_1^- \to 5_1^-$	33·67	53·98	
	$9_1^- \to 7_1^-$	37·08	45·36	
	$11_1^- \to 9_1^-$	20·77	17·75	85 ± 5 [d]
	$1_1^- \to 3_1^-$	—	33·67	
E3	$5_1^- \to 2_1^+$	0·0	27·44	
	$3_1^- \to 0_1^+$	—	0·89	
	$8_1^+ \to 5_1^-$	0·0	0·20	
	$2_2^+ \to 5_1^-$	0·0	46·71	
	$1_1^- \to 4_1^+$	—	3·2	
	$1_1^- \to 2_2^+$	—	2·28	
E4	$1_1^- \to 5_1^-$	—	$1{\cdot}86 \times 10^4$	
	$1_1^- \to 4_2^-$	—	$2{\cdot}10 \times 10^3$	
E5	$5_1^+ \to 0_1^+$	$8{\cdot}11 \times 10^4$	$1{\cdot}23 \times 10^5$	
	$5_1^+ \to 0_2^+$	$9{\cdot}97 \times 10^5$	$1{\cdot}37 \times 10^6$	
M4	$4_1^- \to 0_1^+$	$2{\cdot}3 \times 10^5$	$3{\cdot}6 \times 10^5$	

[a]Papadopoulos *et al* (1975); [b]Stelson and Grodzins (1965); [c]Cochavi *et al* (1971); [d]Lederer *et al* (1971).

transition, the calculated values being $1{\cdot}5 \times 10^5$ and $1{\cdot}17 \times 10^5$ for calculations I and II respectively. These values agree reasonably well with the experimental value $0{\cdot}53 \times 10^5$ (Kocher 1973). Since the $\frac{9}{2_1}^+$ and $\frac{1}{2_1}^-$ states are expected to be single-particle states with very small admixtures of $1p_{3/2}$ and $0f_{5/2}$ excitations, the calculated transition rates are expected to be similar for model spaces I and II.

Table 9. Experimental and calculated electromagnetic transition probabilities of ^{94}Ru. The experimental data are from Lederer *et al* (1971).

Type	$J_i \to J_f$	$B(\sigma, L)_I$	$B(\sigma, L)_{II}$	$B(\sigma, L)_{exp}$
E2	$2_1^+ \to 0_1^+$	71·34	71·92	
	$4_1^+ \to 2_1^+$	72·77	69·48	
	$6_1^+ \to 4_1^+$	27·51	27·13	$2{\cdot}56 \pm 0{\cdot}24$
	$8_1^+ \to 6_1^+$	2·43	2·42	$(9{\cdot}4 \pm 0{\cdot}6) \times 10^{-2}$
	$7_1^- \to 5_1^-$	51·06	77·95	
	$9_1^- \to 7_1^-$	53·86	74·55	
E3	$5_1^- \to 2_1^+$	0·0	28·84	
	$8_1^+ \to 5_1^-$	0·0	6·64	
	$3_1^- \to 0_1^+$	—	15·82	
	$3_1^- \to 2_1^+$	—	654·92	
	$7_1^- \to 4_1^+$	0·0	32·33	
E5	$5_1^- \to 0_1^+$	$9{\cdot}57 \times 10^5$	$1{\cdot}18 \times 10^6$	
	$5_1^- \to 2_1^+$	$0{\cdot}84 \times 10^5$	$1{\cdot}06 \times 10^5$	
	$7_1^- \to 2_1^+$	$0{\cdot}76 \times 10^5$	$1{\cdot}06 \times 10^5$	

Table 10. Experimental and calculated electromagnetic transition probabilities of ^{91}Nb.

Type	$J_i \rightarrow J_f$	$B(\sigma, L)_I$	$B(\sigma, L)_{II}$	$B(\sigma, L)_{exp}$
M1	$\frac{7}{2_1}^+ \rightarrow \frac{9}{2_1}^+$	0·0	$2{\cdot}75 \times 10^{-4}$	
	$\frac{3}{2_1}^- \rightarrow \frac{1}{2_1}^-$	0·0	$1{\cdot}47 \times 10^{-3}$	
	$\frac{3}{2_1}^- \rightarrow \frac{5}{2_1}^-$	$5{\cdot}14 \times 10^{-2}$	$7{\cdot}18 \times 10^{-2}$	
	$\frac{11}{2_1}^- \rightarrow \frac{9}{2_1}^-$	0·0	$5{\cdot}53 \times 10^{-4}$	
	$\frac{11}{2_1}^- \rightarrow \frac{13}{2_1}^-$	$9{\cdot}9 \times 10^{-2}$	$1{\cdot}05 \times 10^{-1}$	
	$\frac{5}{2_2}^- \rightarrow \frac{3}{2_2}^-$	—	$2{\cdot}1 \times 10^{-3}$	
E2	$\frac{13}{2_1}^- \rightarrow \frac{9}{2_1}^+$	30·96	38·40	
	$\frac{17}{2_1}^+ \rightarrow \frac{13}{2_1}^+$	31·60	41·93	
	$\frac{21}{2_1}^+ \rightarrow \frac{17}{2_1}^+$	20·30	19·57	106 ± 11[a]
	$\frac{7}{2_2}^- \rightarrow \frac{3}{2_1}^-$	—	0·39	
	$\frac{7}{2_2}^- \rightarrow \frac{3}{2_2}^-$	—	90·04	
	$\frac{5}{2_1}^- \rightarrow \frac{1}{2_1}^-$	28·00	64·32	
	$\frac{5}{2_2}^- \rightarrow \frac{1}{2_1}^-$	—	0·82	
	$\frac{5}{2_2}^- \rightarrow \frac{9}{2_1}^-$	—	0·19	
	$\frac{9}{2_1}^- \rightarrow \frac{5}{2_1}^-$	28·15	69·68	<178[b]
	$\frac{11}{2_1}^- \rightarrow \frac{7}{2_1}^-$	—	33·02	
	$\frac{13}{2_1}^- \rightarrow \frac{9}{2_1}^-$	27·10	30·0	$68{\cdot}8 \pm 3{\cdot}1$[c]
	$\frac{17}{2}^- \rightarrow \frac{13}{2_1}^-$	10·78	6·73	$32{\cdot}0 \pm 1{\cdot}9$[d]
E3	$\frac{7}{2_1}^+ \rightarrow \frac{1}{2_1}^-$	0·0	64·16	
	$\frac{11}{2_1}^+ \rightarrow \frac{5}{2_1}^-$	0·0	47·36	
	$\frac{13}{2_1}^- \rightarrow \frac{9}{2_1}^+$	0·0	3·43	
M4	$\frac{1}{2_1}^- \rightarrow \frac{9}{2_1}^+$	$3{\cdot}16 \times 10^5$	$4{\cdot}04 \times 10^5$	$2{\cdot}60 \times 10^5$[b]

[a]Schneider *et al* (1975); [b]Verheul and Ewbank (1972); [c]Baba *et al* (1976); [d]Brown *et al* (1976).

The transition probabilities of ^{91}Nb are listed in table 10. The calculated E2 transition probabilities are usually smaller than the observed values. However, the calculated values seem to have the correct order of magnitude. The calculated M4 transition probability agrees reasonably well with the experimental value (Verheul and Ewbank 1972). In general, except for the transitions that are forbidden in model space I, it seems that expansion of the model space does not produce a significant change in the calculated transition probabilities of ^{91}Nb. Some E2 transitions which are not available in model space I are also calculated for reference. The calculation shows that the $\frac{5}{2_2}^- \rightarrow \frac{1}{2_1}^-, \frac{9}{2}^-$ E2

Table 11. Experimental and calculated electromagnetic transition probabilities of ^{93}Tc.

Type	$J_i \rightarrow J_f$	$B(\sigma, L)_I$	$B(\sigma, L)_{II}$	$B(\sigma, L)_{exp}$
M1	$\frac{7}{2_1}^+ \rightarrow \frac{9}{2_1}^+$	0·0	$4{\cdot}23 \times 10^{-5}$	
	$\frac{11}{2_1}^+ \rightarrow \frac{9}{2_1}^+$	0·0	$2{\cdot}63 \times 10^{-5}$	
	$\frac{3}{2_1}^- \rightarrow \frac{1}{2_1}^-$	0·0	$1{\cdot}62 \times 10^{-3}$	
	$\frac{3}{2_1}^- \rightarrow \frac{5}{2_1}^-$	0·0	$3{\cdot}81 \times 10^{-3}$	
E2	$\frac{7}{2_1}^+ \rightarrow \frac{9}{2_1}^+$	$3{\cdot}2 \times 10^{-3}$	1·05	
	$\frac{17}{2_1}^+ \rightarrow \frac{13}{2_1}^+$	4·67	12·06	
	$\frac{21}{2_1}^+ \rightarrow \frac{17}{2_1}^+$	25·04	29·06	$65{\cdot}9 \pm 4{\cdot}0$[a]
	$\frac{25}{2_1}^+ \rightarrow \frac{21}{2_1}^-$	33·37	41·95	
	$\frac{21}{2_1}^- \rightarrow \frac{17}{2_1}^-$	44·51	60·43	
	$\frac{17}{2_1}^- \rightarrow \frac{13}{2_1}^-$	8·12	12·37	$11{\cdot}4 \pm 0{\cdot}9$[b]
M4	$\frac{1}{2_1}^- \rightarrow \frac{9}{2_1}^+$	$3{\cdot}99 \times 10^5$	$4{\cdot}20 \times 10^5$	$4{\cdot}21 \times 10^5$[c]

[a]Schneider *et al* (1975); [b]Brown *et al* (1976a); [c]Kocher (1972).

transitions are rather weak compared with other E2 transitions. The $\frac{7}{2}_2^- \rightarrow \frac{3}{2}_1^-$ E2 transition is also quite weak while the $\frac{7}{2}_2^- \rightarrow \frac{3}{2}_2^-$ E2 transition is rather strong. This is because $\frac{7}{2}_2^+$ is a $(1p_{3/2})^{-1}$ dominated state and $\frac{3}{2}_2^-$ has a rather strong $(1p_{3/2})^{-1}$ admixture, while the $\frac{3}{2}_1^-$ state does not have such admixtures.

The transition probabilities of ^{93}Tc are listed in table 11. The calculated $\frac{21}{2}_1^+ \rightarrow \frac{17}{2}_1^+$ and $\frac{17}{2}_1^- \rightarrow \frac{13}{2}_1^-$ E2 transition probabilities agree quite well with the experimental values (Schneider *et al* 1975, Brown *et al* 1976b). The M4 transition probability between $\frac{1}{2}_1^-$ and $\frac{9}{2}_1^+$ states can be reproduced quite well in both model-space calculations. In general, expansion of the model space seems to improve the agreement between the calculated and experimental values.

6. Conclusions

By using a two-range central-plus-tensor potential, the effects of $1p_{3/2}$ and $0f_{5/2}$ excitations are studied for $N = 50$ isotones. It is found that by expanding the model space to include $1p_{3/2}$ and $0f_{5/2}$ one-hole excitations, many more low-lying levels can be accommodated in the model. Expansion of the model space has rather strong effects on the low-lying level spectra of ^{89}Y, ^{90}Zr and ^{91}Nb while it has much a weaker effect on ^{92}Mo, ^{93}Tc and ^{94}Ru. For ^{89}Y, ^{90}Zr and ^{91}Mo 25 levels are found to have strong $1p_{3/2}$ and $0f_{5/2}$ admixtures while for ^{92}Mo, ^{93}Tc and ^{94}Ru very few levels have strong $1p_{3/2}$ and $0f_{5/2}$ admixtures. In the calculations we found that the $1p_{3/2}$ excitation is more important than the $0f_{5/2}$ excitation. However, some levels do have strong $0f_{5/2}$ admixtures. In particular, it was found that the $\frac{5}{2}_1^-$ and $\frac{11}{2}_2^+$ states of ^{89}Y, the 6_1^- and 7_1^- states of ^{90}Zr, the $\frac{5}{2}_2^-$ state of ^{91}Nb and the 1_1^- state of ^{92}Mo are all dominated by $0f_{5/2}$ excitation.

The best-fit effective potentials are used to calculate the two-body matrix elements. It was found that the matrix elements for $1p_{1/2}$ and $0g_{9/2}$ are quite similar for the two choices of model space. In the calculation with model space II matrix elements with $1p_{3/2}$ and $0f_{5/2}$ excitations are also produced for reference. The resultant wavefunctions are used to calculate various type of transition probabilities. Naturally, the expanded model space gives many transitions that are strictly forbidden in the smaller model space. For those transitions that are not forbidden by model space I expansion of the model space usually improves the agreement with experimental data. However, the discrepancies between the calculated and experimental results are usually large compared with the amount of improvement. This seems to indicate that further expansion of the model space, such as two-hole excitations in $1p_{3/2}$ and $0f_{5/2}$ orbitals, is still needed. In fact, even in model space II the 3_1^- state of ^{90}Zr and the 0_2^+ states of ^{92}Mo and ^{94}Ru cannot be fitted. These states may have much more complicated structure.

Since we have performed a least-squares-fit calculation on the energy spectra, it is not surprising that the calculation is more successful in explaining energy spectra than transition probabilities. The least-squares-fit calculation with mixed input data with both energy levels and transition rates as suggested by Gloeckner and Serduke (1974) is very interesting. Experimental data on transition rates are meagre and not so reliable as those on energy levels. Therefore, it may not be proper to perform an overall least-squares-fit calculation with mixed input data at present. If more reliable data on transition rates become available in the future, a calculation with mixed input data in a further expanded model space will certainly give us more conclusive information on the properties of $N = 50$ isotones.

Acknowledgment

The authors wish to thank Professors S T Hsieh and D S Chuu for helpful discussions.

References

Anantaraman N and Schiffer J P 1971 *Phys. Lett.* **37B** 229–32
Auerbach N and Talmi I 1965 *Nucl. Phys.* **64** 458–80
Baba C V K, Fossan D B, Faestermann T, Feilitzsch F, Maier M R, Raghavan P, Raghavan R S and Signorini C 1976 *Nucl. Phys.* A **257** 135–43
Ball J B, McGrory J B and Larsen J S 1972 *Phys. Lett.* **41B** 581–4
Bauer R, Ring P and Speth J 1973 Contribution to the *Int. Conf. on Nuclear Physics, Munich* p 106
Bayman B F, Reiner A S and Sheline R K 1959 *Phys. Rev.* **115** 1627–35
Bellicard J, Leconte P, Curtis T H, Eisenstein R A, Madsen D and Bockelman C 1970 *Nucl. Phys.* A **143** 213–24
Beshai S̈, Fransson N, Froberg L E and Sundstrom B 1978 *Nucl. Phys.* A **296** 151–9
Brown B A, Fossan D B, Lesser P M S and Poletti A R 1976a *Phys. Rev.* C **13** 1194–9
Brown B A, Lesser P M S and Fossan D B 1976b *Phys. Rev.* C **13** 1900–21
Chapman R, Kitching J E and McLatchie W 1972 *Nucl. Phys.* A **196** 347–52
Chiang H C, Hsieh S T, Chuu D S and Han C S 1978 *Phys. Rev.* C **18** 2756–64
Cochavi S, McDonald J M and Fossan D B 1971 *Phys. Rev.* C **3** 1352–61
Cohen S, Lawson R D, Macfarlane M H and Soga M 1964 *Phys. Lett.* **10** 195–8
Dedes C and Irvine J M 1975 *J. Phys. G: Nucl. Phys.* **1** 865–73
Fivozinsky S P, Penner S, Lightbody J M Jr and Bulm D 1974 *Phys. Rev.* C **9** 1533–42
Fujita D K and Komoda T 1978 *Prog. Theor. Phys.* **60** 178–96
Glickstein S S, Tessler G and Goldsmith M 1971 *Phys. Rev.* C **4** 1818–28
Gloeckner D H, Macfarlane M H, Lawson R D and Serduke F J D 1972 *Phys. Lett.* **40B** 597–601
Gloeckner D H and Serduke F J D 1974 *Nucl. Phys.* A **220** 477–90
Grecescu M, Nilsson A and Harms-Ringdahl L 1973 *Nucl. Phys.* A **212** 429–46
Ho P X, Bellicard J, Leconte P and Sick I 1973 *Nucl. Phys.* A **210** 189–210
Horton J L, Hollas C L, Riley P J, Zaidi S A A, Jones C M and Ford J L C Jr 1972 *Nucl. Phys.* A **190** 362–72
Hughes T A 1969 *Proc. Int. Conf. on Properties of Nuclear States, Montreal* ed M Harvey *et al* p 728
Hulstman L, Blok H P, Verburg J, Hoogteyling J G, Nederveen C B, Vijlbrief H T, Kaptein E J, Milo S W L and Blok J 1975 *Nucl. Phys.* A **251** 269–88
King Yen M M, Hsieh S T, Wang M C and Chiang H C 1977 *Lett. Nuovo Cim.* **19** 432–6
Kocher D C 1972 *Nuclear Data Sheets* B **8** 527–98
—— 1973 *Nuclear Data Sheets* **10** 241–308
——1975 *Nuclear Data Sheets* **16** 445–505
Kuo T T S and Brown G E 1968 *Nucl. Phys.* A **114** 241–79
Lederer C M, Jaklevic J M and Hollander J M 1971 *Nucl. Phys.* A **169** 449–88
Löbner K E G 1964 *Nucl. Phys.* **58** 49–55
Metzger F R 1977 *Phys. Rev.* C **15** 193–5
Moinester M, Schiffer J P and Alford W P 1969 *Phys. Rev.* **179** 984–95
Papadopoulos C T, Hartas A G, Assimakopoulos P A, Andritsopoulos G and Gangas N H 1975 *Nucl. Phys.* A **254** 93–109
Riley P J, Horton J L, Hollas C L, Zaidi S A A, Jones C M and Ford J L C Jr 1971 *Phys. Rev.* C **4** 1864–76
Schäfer W and Rauch F 1977 *Nucl. Phys.* A **291** 165–82
Schiffer J P and True W W 1976 *Rev. Mod. Phys.* **48** 191–217
Schneider W D, Gonsior N H and Günther C 1975 *Nucl. Phys.* A **249** 103–10
Shamai Y, Ashery O, Yavin A I, Bruge G and Chaumeaux A 1972 *Nucl. Phys.* A **197** 211–28
Singhal R P, Brain S W, Gillespie W A, Johnston A, Lees E W and Slight A G 1974 *Nucl. Phys.* A **218** 189–200
Stelson P H and Grodzins L 1965 *Nuclear Data* A **1** 21–102
Stooksberry R W, Anderson J H and Goldsmith M 1976 *Phys. Rev.* C **13** 1061–71
Tucker A B and Simmons S O 1970 *Nucl. Phys.* A **156** 83–92
Talmi I and Unna I 1960 *Nucl. Phys.* **19** 225–42
Thornton S T, Gustafson D E, Ford J L C Jr, Toth K S and Hensley D C 1976 *Phys. Rev.* C **13** 1502–9
Verheul H and Ewbank W B 1972 *Nuclear Data Sheets* B **8** 477–526
Vervier J 1966 *Nucl. Phys.* **75** 17–78